

PAPER • OPEN ACCESS

Finite Element Stress Analysis of Acrylic with Embedded Optical Fibre Sensors

To cite this article: O Kurdi *et al* 2020 *IOP Conf. Ser.: Mater. Sci. Eng.* **807** 012018

View the [article online](#) for updates and enhancements.

You may also like

- [Development and modeling of multi-phase polymeric origami inspired architecture by using pre-molded geometrical features](#)
Mohamed Ali E Kshad and Hani E Naguib
- [Optimization of heat transfer properties of the directional solidification furnace by modifying heat exchanger blocks](#)
Kesavan V, Srinivasan M and Ramasamy P
- [Studying The Influence Of Hydrostatic Pressure On The Plastic Deformation Of Large Water Tanks](#)
Hasan Shakir Majdi, Auday Shaker Hadi, Laith Jaafer Habeeb et al.



ECS The Electrochemical Society
Advancing solid state & electrochemical science & technology

242nd ECS Meeting

Oct 9 – 13, 2022 • Atlanta, GA, US

Early hotel & registration pricing ends September 12

Presenting more than 2,400 technical abstracts in 50 symposia

The meeting for industry & researchers in

BATTERIES
ENERGY TECHNOLOGY
SENSORS AND MORE!

 Register now!

  **ECS Plenary Lecture featuring M. Stanley Whittingham,**
Binghamton University
Nobel Laureate –
2019 Nobel Prize in Chemistry



Finite Element Stress Analysis of Acrylic with Embedded Optical Fibre Sensors

O Kurdi^{1,2*}, S A Widyanto¹, G D Haryadi^{1,2}, A Suprihanto¹, I Yulianti³, A Rahman¹

¹Mechanical Engineering Department, Diponegoro Universiti, Semarang, Central Java, Indonesia

²National Center for Sustainable Transportation Technology, Indonesia

³Physics Department, Universitas Negeri Semarang, Central Java, Indonesia

Corresponding e-mail: ojokurdi@ft.undip.ac.id

Abstract. Finite element (FE) techniques are used to analyse mechanical stress in optical fibre sensors embedded in acrylic. The models represent many features observed in real materials with embedded fibre optic for stress and strain sensor application such as for health monitoring of structures. Three thicknesses, namely 6 mm, 8 mm and 10 mm of acrylic were analyzed with the optical fibre embedded at the mid-plane of acrylic. The simulation was done by implementing Finite Element Method using ABAQUS software. Contact between acrylic and optical fibre was modelled as frictionless and with friction. The friction coefficient was varied for various values which are 0.3, and 0.5. This paper investigates the effect of friction coefficient and the effect of fibre optic's depth embedded in acrylic to the their von Misses stress. Simulation result shows that the higher the friction coefficient the higher von Misses stress in fibre optic and the higher von Misses stress in acrylic. The higher the fibre's depth the higher von Misses stress in fibre and the lower von Misses stress in acrylic. The maximum stress occurred for the coefficient of friction 0.5, with magnitude of 116.4 MPa and 58.72 MPa for acrylic and optical fibre respectively. The most significant effect of fibre's depth to the von Misses stress was obtained for 1 mm depth for acrylic and 5 mm for optical fibre, with magnitude of 72.64 MPa and 57.65 MPa for acrylic and optical fibre respectively.

1. Introduction

Fibre optic as sensor has many advantages namely: small size, light weight and immunity to electromagnetic interference [1]. Fibre optic sensor with these advantages can be embedded into the host material to form an ideally smart structure system. Nowadays fibre optic has been used as sensor in many applications such as for structural health monitoring and aerospace engineering, industrial processing and defence industry [2-8]. The information on numerous important parameters such as micro strain, micro vibration, and stiffness, which are vital to the in situ structural health monitoring as well as the optimizations of the system performances can be obtain from embedded fibre optic sensor [9-18].

Fibre optic has been embedded in some material as a pressure sensor in health monitoring of structures and bridges. Acrylic has been used widely for roof and wall of some buildings. Therefore, to ensure the safety of fibre optic that embedded in acrylic it is necessary to investigate the stress condition inside the fibre optic under pressure load. Some researchers have carried out the stress analysis embedded in composites and other materials [3], [11-12], [14-16], [19-24]. The contact condition between fibre optic and acrylic has also been defined and varied as frictionless and with certain various



friction coefficient, namely 0.3, 0.5 and 0.8. The depth of fibre optic embedded in acrylic also will be varied by 1mm until 5 mm. The effect of friction coefficient and the depth of fibre optic was embedded in acrylic will be investigated in this research using FE simulation technique.

2. Finite Element Simulation

2.1. Acrylic and fibre optic model

Model of of fibre optic embedded in acrylic has been drawn using Solid works software. The model depicted in Figure 1, for acrylic and fibre optic respectively. The fibre optic was modelled as a solid rod with diameter of 1 mm, and the acrylic has a 50 mm in length and 40 mm in width, with various of thicknesses, 6 mm, 8 mm and 10 mm. The material properties of acrylic and fibre optic were shown in Table 1.

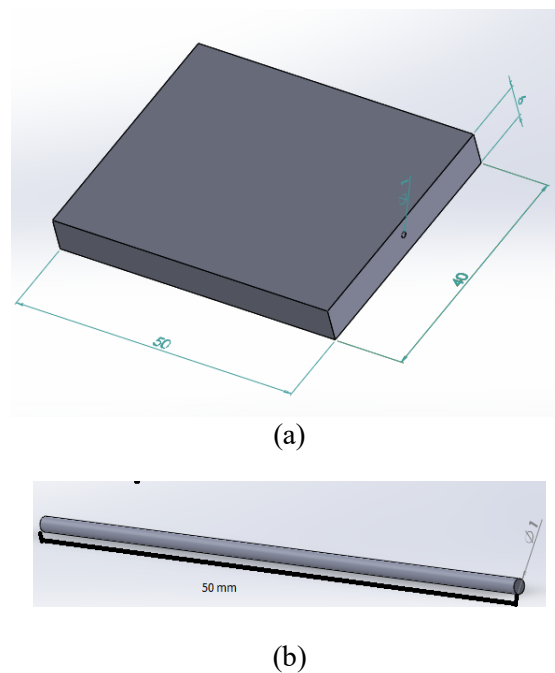


Figure 1. Model (a) Acrylic; (b) fibre optic

Table 1. Properties of acrylic and fibre

Mechanical Property	Material	
	Fibre Optic	Acrylic
Density (kg/m ³)	7200	7850
Ultimate Tensile Strength (MPa)	450	450
Tensile Yield Strength (MPa)	280	435
Modulus of Elasticity (MPa)	140	190
Poisson's Ratio	0.211	0.27

2.2. Load and boundary condition

Load was given as distributed pressure on top of surface of acrylic with fibre optic has embedded inside. The magnitude of pressure is 80 MPa. That magnitude was considered according to maximum pressure that can be applied to the acrylic with has 6 mm in thickness.

There are two boundary conditions (BCs) on the model. First boundary condition is fixed that was applied in the bottom of the acrylic, this BC restricted the model to translate and rotate in all directions. The second BC was applied on both of two ends of fibre. This kind of BC restricted the fibre translation in axial direction and restricted rotation in all directions. Figure 2 show the load and two boundary conditions of the model.

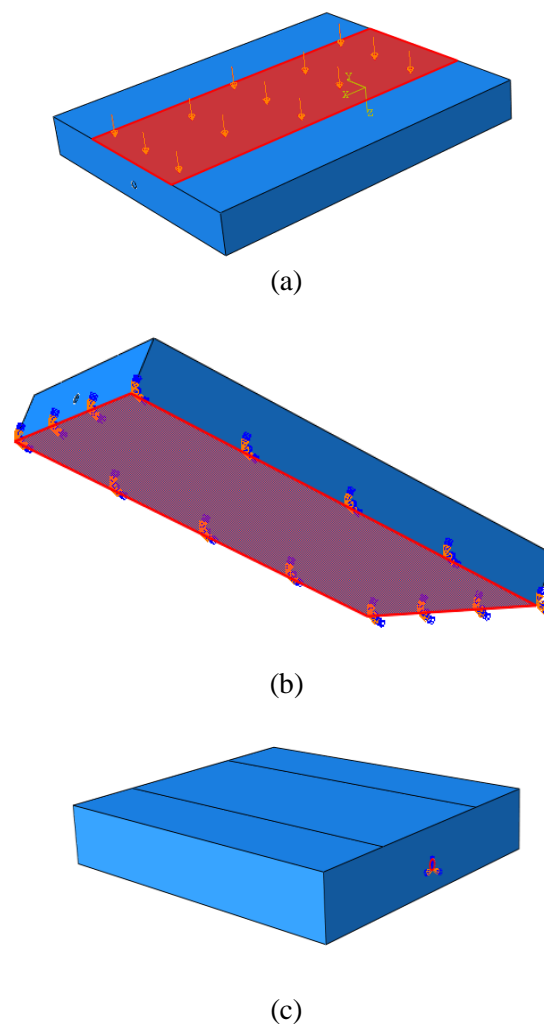
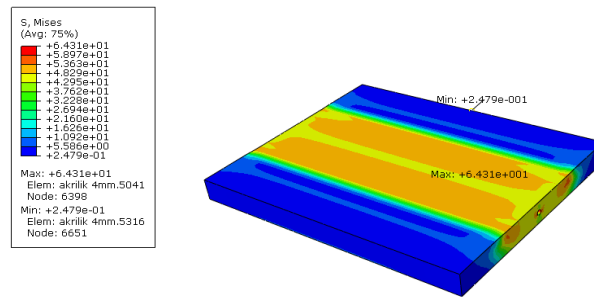


Figure 2. Load and Boundary Condition; (a) Load; (b) BC 1; (c) BC 2

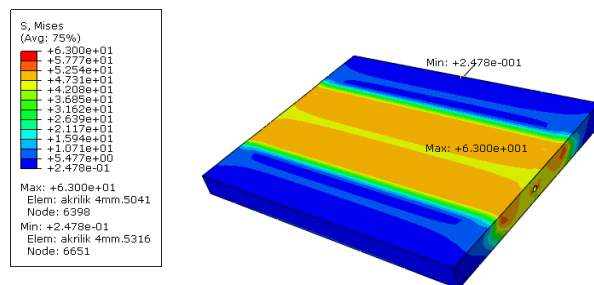
3. Result and Discussion

The simulation result of von Misses stress for fibre with various coefficients of friction were shown in Figure 3 for 4 mm thickness of acrylic and 1 mm of fibre's depth. The maximum von Misses stress of acrylic for frictionless contact condition is 64,04 MPa, while the von Misses stress for coefficient of

friction 0.3 is 116.4 MPa. The von Misses stress of acrylic tend to increase by increasing the coefficient of friction.



(a)



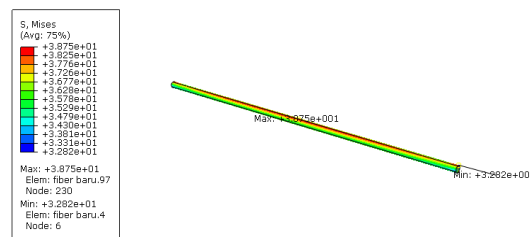
(b)

Figure 3. Von Misses stress in acrylic of 4 mm acrylic thickness; (a). for frictionless condition; (b). for 0.3 coefficient of friction

Von Misses stress simulation result for 4 mm thickness of acrylic and 1 mm of fibre’s depth can be seen in Figure 4. The trend of stress in the fibre also same with that of stress in the acrylic. The stress is increase by increasing of coefficient of friction.



(a)



(b)

Figure 4. Von Misses stress in fibre of 4 mm acrylic thickness; (a). for frictionless condition; (b). for 0.3 coefficient of friction.

The relation between von Misses stress and the coefficient of friction was stated in Figure 5. The von Misses stress of both acrylic and fibre were increase by increasing of coefficient of friction.

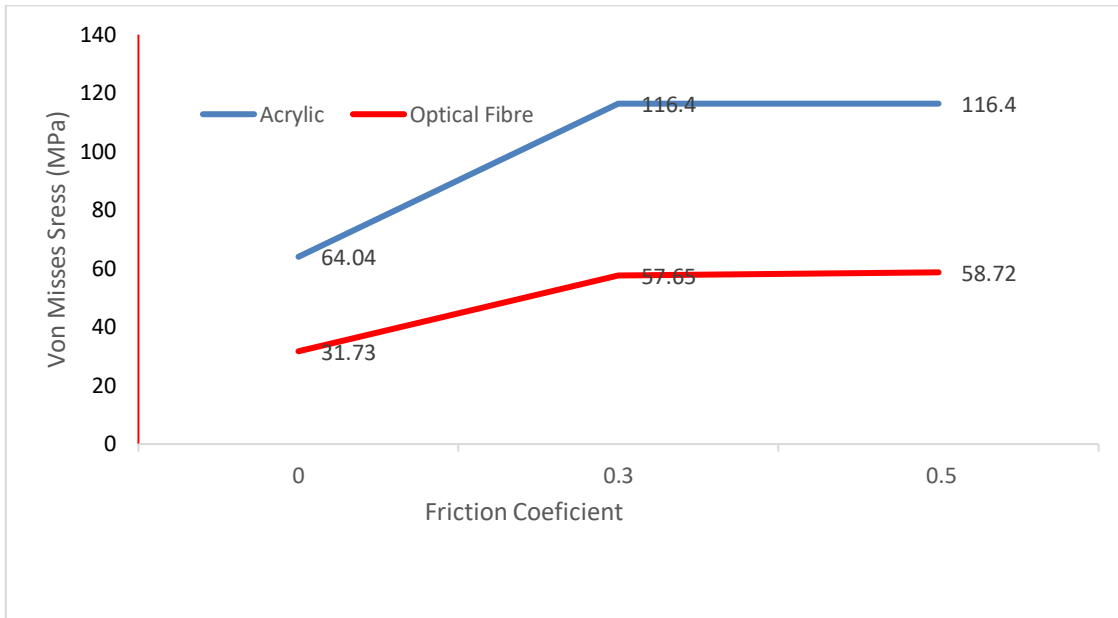
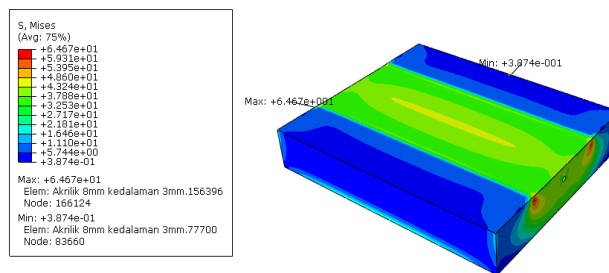
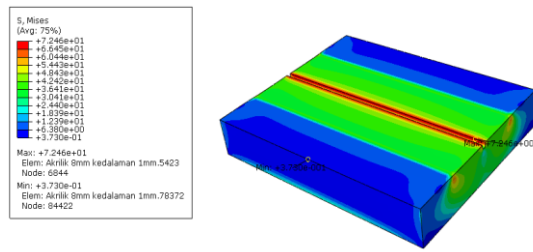


Figure 5. Effect of the coefficient of friction to the stress in fibre optic and acrylic for 1 mm depth.

Figure 6 shows the von Misses stress of acrylic for 8 mm thickness of acrylic and 3 mm of fibre’s depth, frictionless condition. It can be seen that the maximum von Misses stress was occurred at near of surface with magnitude of 64.67 MPa, while the acrylic with 1 mm of fibre’s depth has the von Misses stress of 72.46 MPa which occurred at the surface of acrylic which contact with fibre.



(a)



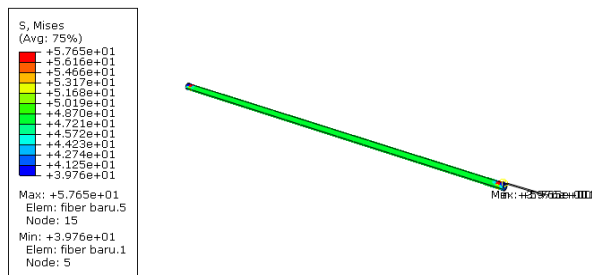
(b)

Figure 6. Von Misses stress in acrylic of 8 mm acrylic thickness (frictionless); (a). for 3 mm of fibre’s depth; (b). for 1 mm of fibre’s depth

Figure 7 shows the von Misses stress of fibre for 8 mm thickness of acrylic and 3 mm of fibre’s depth, frictionless condition. It can be seen that the maximum von Misses stress was occurred at surface near to the right end of fibre with magnitude of 70.32 MPa, while the fibre with 1 mm of fibre’s depth has the von Misses stress of 57.65 MPa which occurred at the same region with that of 3 mm of fibre’s depth.



(a)



(b)

Figure 7. Von Misses stress in fibre of 8 mm acrylic thickness (frictionless); (a). for 3 mm of fibre’s depth; (b). for 1 mm of fibre’s depth

The relation between von Misses stress and the fibre’s depth was displayed in Figure 8. The von Misses stress of fibre was increase by increasing of fibre’s depth, but The von Misses stress of acrylic was decrease by increasing of fibre’s depth.

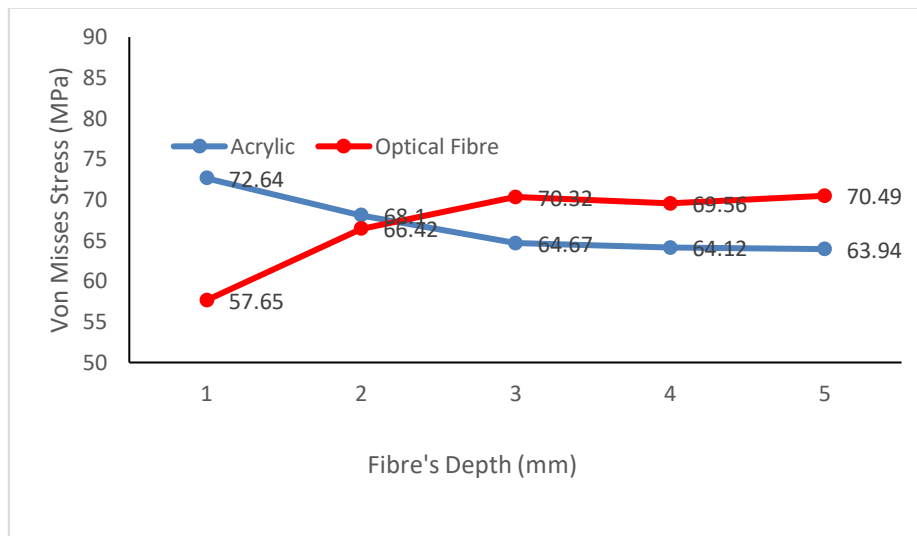


Figure 8. Effect of the fibre's depth to the stress in fibre optic and acrylic for frictionless condition.

4. Conclusion

The stress analysis of fibre optic sensor embedded in acrylic was accomplished by finite element method. Based on the simulation result, it can be concluded that von Mises stress of fibre optic and acrylic were increase by increasing of coefficient of friction. The von Mises stress of fibre was increase by increasing of fibre's depth, but The von Mises stress of acrylic was decrease by increasing of fibre's depth. The maximum von Mises stress of acrylic and optical fibre sensor was occurred for the coefficient of friction of 0.5, for 1 mm depth the magnitude of stress is 116.4 MPa and 58.72 MPa for acrylic and optical fibre respectively. The maximum von Mises stress for fibre's depth variation was occurred at 1 mm for acrylic and 5 mm depth for optical fibre, with magnitude of 72.64 MPa and 57.65 MPa for acrylic and optical fibre respectively.

Acknowledgments

The authors gratefully acknowledge partial funding support from the USAID under the SHERA program.

References

- [1] K. T. V. Grattan and T. Sun, "Fibre optic sensor technology: an overview," *Sensors Actuators A Phys.*, vol. 82, no. 1–3, pp. 40–61, May 2000.
- [2] T. H. T. Chan *et al.*, "Fibre Bragg grating sensors for structural health monitoring of Tsing Ma bridge: Background and experimental observation," *Eng. Struct.*, vol. 28, no. 5, pp. 648–659, Apr. 2006.
- [3] L. P. Canal, R. Sarfaraz, G. Violakis, J. Botsis, V. Michaud, and H. G. Limberger, "Monitoring strain gradients in adhesive composite joints by embedded fibre Bragg grating sensors," *Compos. Struct.*, vol. 112, pp. 241–247, Jun. 2014.
- [4] H.-N. Li, D.-S. Li, and G.-B. Song, "Recent applications of fibre optic sensors to health monitoring in civil engineering," *Eng. Struct.*, vol. 26, no. 11, pp. 1647–1657, Sep. 2004.
- [5] M. Majumder, T. K. Gangopadhyay, A. K. Chakraborty, K. Dasgupta, and D. K. Bhattacharya, "Fibre Bragg gratings in structural health monitoring—Present status and applications," *Sensors Actuators A Phys.*, vol. 147, no. 1, pp. 150–164, Sep. 2008.
- [6] Z. DjinoVIC, M. Tomic, and C. Gamauf, "Fibre-optic interferometric sensor of magnetic field for structural health monitoring," *Procedia Eng.*, vol. 5, pp. 1103–1106, Jan. 2010.
- [7] J. Alvarez-Montoya, A. Carvajal-Castrillón, and J. Sierra-Pérez, "In-flight and wireless damage detection in a UAV composite wing using fibre optic sensors and strain field pattern recognition," *Mech. Syst. Signal Process.*, vol. 136, p. 106526, Feb. 2020.

- [8] C. Du, S. Dutta, P. Kurup, T. Yu, and X. Wang, "A review of railway infrastructure monitoring using fibre optic sensors," *Sensors Actuators A Phys.*, p. 111728, Nov. 2019.
- [9] L. Rodriguez-Cobo, A. Cobo, and J.-M. Lopez-Higuera, "Embedded compaction pressure sensor based on Fibre Bragg Gratings," *Measurement*, vol. 68, pp. 257–261, May 2015.
- [10] A. Y. Fedorov, N. A. Kosheleva, V. P. Matveenکو, and G. S. Serovaev, "Strain measurement and stress analysis in the vicinity of a Fibre Bragg grating sensor embedded in a composite material," *Compos. Struct.*, p. 111844, Jan. 2020.
- [11] D. C. Lee, J. J. Lee, and S. J. Yun, "The mechanical characteristics of smart composite structures with embedded optical fibre sensors," *Compos. Struct.*, vol. 32, no. 1–4, pp. 39–50, Jan. 1995.
- [12] N. Lammens, G. Luyckx, E. Voet, W. Van Paepegem, and J. Degrieck, "Finite element prediction of resin pocket geometry around embedded optical fibre sensors in prepreg composites," *Compos. Struct.*, vol. 132, pp. 825–832, Nov. 2015.
- [13] D. Savastru, S. Miclos, R. Savastru, and I. I. Lancranjan, "Study of thermo-mechanical characteristics of polymer composite materials with embedded optical fibre," *Compos. Struct.*, vol. 183, pp. 682–687, Jan. 2018.
- [14] P. Zhu, X. Xie, X. Sun, and M. A. Soto, "Distributed modular temperature-strain sensor based on optical fibre embedded in laminated composites," *Compos. Part B Eng.*, vol. 168, pp. 267–273, Jul. 2019.
- [15] S. Miclos, D. Savastru, R. Savastru, and I. I. Lancranjan, "Transverse mechanical stress and optical birefringence induced into single-mode optical fibre embedded in a smart polymer composite material," *Compos. Struct.*, vol. 218, pp. 15–26, Jun. 2019.
- [16] R. Prussak, D. Stefaniak, E. Kappel, C. Hühne, and M. Sinapius, "Smart cure cycles for fibre metal laminates using embedded fibre Bragg grating sensors," *Compos. Struct.*, vol. 213, pp. 252–260, Apr. 2019.
- [17] M. Koerd *et al.*, "Fabrication and characterization of Bragg gratings in perfluorinated polymer optical fibres and their embedding in composites," *Mechatronics*, vol. 34, pp. 137–146, Mar. 2016.
- [18] J. Peng, S. Jia, Y. Jin, S. Xu, and Z. Xu, "Design and investigation of a sensitivity-enhanced fibre Bragg grating sensor for micro-strain measurement," *Sensors Actuators A Phys.*, vol. 285, pp. 437–447, Jan. 2019.
- [19] Y. Yu, B. Zhang, Z. Tang, and G. Qi, "Stress transfer analysis of unidirectional composites with randomly distributed fibres using finite element method," *Compos. Part B Eng.*, vol. 69, pp. 278–285, Feb. 2015.
- [20] D. Li, Q.-S. Yang, X. Liu, and X.-Q. He, "Experimental and cohesive finite element investigation of interfacial behavior of CNT fibre-reinforced composites," *Compos. Part A Appl. Sci. Manuf.*, vol. 101, pp. 318–325, Oct. 2017.
- [21] R. M. Measures, "Fibre optic sensing for composite smart structures," *Compos. Eng.*, vol. 3, no. 7–8, pp. 715–750, Jan. 1993.
- [22] M A Pulungan, Sutikno and M S M Sani "Analysis of Bulletproof Vest Made from Fiber Carbon Composite and Hollow Glass Microsphere (HGM) in Absorbing Energy due to Projectile Impact" IOP Conf. Ser. Mater. Sci. Eng. 206 012001, 2019
- [23] M S M Sani, N A Z Abdullah, S N Zahari, J P Siregar and M M Rahman "Finite element model updating of natural fibre reinforced composite structure in structural dynamics" MATEC Web of Conferences 83 03007, 2016
- [24] R M Yaacob, M A H Hashim and M S M Sani "Finite element modeling and updating of the composite plate structure" IOP Conf. Ser. Mater. Sci. Eng. 100 01201, 2019